JACS
JOURNAL OF THE AMERICAN CHEMICAL SOCIETY

COMMUNICATION

pubs.acs.org/JACS

$Na_2CsBe_6B_5O_{15}$: An Alkaline Beryllium Borate as a Deep-UV Nonlinear Optical Crystal

Shichao Wang and Ning Ye*

Key Laboratory of Optoelectronic Materials Chemistry and Physics, Fujian Institute of Research on the Structure of Matter, Chinese Academy of Sciences, Fuzhou, Fujian 350002, P. R. China

Supporting Information

ABSTRACT: A new deep-UV nonlinear optical crystal, $Na_2CsBe_6B_5O_{15}$, has been grown through spontaneous crystallization with a molten flux based on $Na_2O-Cs_2O-B_2O_3$. $Na_2CsBe_6B_5O_{15}$ contains two-dimensional alveolate beryllium borate layers $[Be_2BO_5]_\infty$ that are bridged via planar $[BO_3]$ groups. UV−vis diffuse reflectance analysis on a powder sample of $Na_2CsBe_6B_5O_{15}$ indicates that the short-wavelength absorption edge of $Na_2CsBe_6B_5O_{15}$ is below 200 nm. Second-harmonic generation (SHG) on the powder sample was measured with a 1064 nm laser using the Kurtz and Perry technique, which showed that $Na_2CsBe_6B_5O_{15}$ is a phase-matchable material, and its measured SHG coefficient is ~1.17 times as large as the d_{36} coefficient of potassium dihydrogen phosphate. The relatively larger SHG coefficient of $Na_2CsBe_6B_5O_{15}$ originates from its shorter distance between the adjacent layers bridged via the small $[BO_3]$ groups.

Deep-UV nonlinear optical (NLO) crystals that can produce deep-UV coherent light with wavelengths below 200 nm have become increasingly important and are attracting more attention because of their promising applications in photonic technologies over the past decade.[1−8] In spite of many reports in the literature,[4,6] it remains challenging to obtain practically useful materials possessing high NLO coefficients and wide UV transparency, especially those covering the deep-UV region. Currently, the exploration of such crystals is mainly focused on alkali- and alkaline-earth-metal beryllium borates that exhibit short transmission cutoff wavelengths in the UV region, such as $ABe_2BO_3F_2$ (A = Na, K, Rb, Cs, Tl)[1−5] and $M_2Be_2B_2O_7$[6−8] (M = Sr, Ba). On the basis of the relationship between the structure and overall NLO properties, there are two approaches for producing large NLO effects: (1) choosing favorable structural units and having them aligned parallel[9−15] and (2) increasing the density of the NLO structural units. In our previous study, we reported the structural design and preparation of a series of new unitary alkali-metal beryllium borates with stoichiometries of β-$KBe_2B_3O_7$, $RbBe_2B_3O_7$, and γ-$KBe_2B_3O_7$[16] that consist of two-dimensional (2D) alveolate beryllium borate layers, $[Be_2BO_5]_\infty$, bridged via flexible one-dimensional (1D) $[BO_2]_\infty$ chains or rigid, planar $[B_3O_6]$ groups. The strong connections provided by the covalent bonds between layers mitigate drawbacks such as layer growth habit and cleavage, which have limited the optical applications of $KBe_2BO_3F_2$ (KBBF) crystals. Meanwhile, the distances between adjacent layers in β-$KBe_2B_3O_7$ (8.73 Å), $RbBe_2B_3O_7$ (8.86 Å), and γ-$KBe_2B_3O_7$ (8.70 Å) are longer than that in KBBF (6.25 Å), resulting in a lower $[BO_3]$ density in the former. Therefore, the SHG coefficients of β-$KBe_2B_3O_7$, $RbBe_2B_3O_7$, and γ-$KBe_2B_3O_7$ were found to be smaller than that of KBBF. In our continued quest for large SHG effects in these layered compounds containing alveolate networks, we tried to construct their structures through the introduction of smaller $[BO_3]$ groups to serve as bridges in order to increase their $[BO_3]^{3-}$ densities. One of the resulting alkaline beryllium borates, $Na_2CsBe_6B_5O_{15}$, was found in this work to exhibit a shorter interlayer distance, and consequently, a larger SHG effect was obtained through proper allocation of binary alkaline cations to fit the cavities between adjacent layers.

Because of the high toxicity of the beryllium oxide powders upon inhalation, all of the experiments were performed under sufficient ventilation. Single crystals of $Na_2CsBe_6B_5O_{15}$ were grown from a high-temperature solution using $Na_2O-Cs_2O-B_2O_3$ as a flux. This solution was prepared in a platinum crucible after melting of a mixture of Na_2CO_3, Cs_2CO_3, BeO, and B_2O_3 having a $Na_2O/Cs_2O/BeO/B_2O_3$ molar ratio of 2:3:4:9. The mixture (10 g) was heated in a temperature-programmable electric furnace at 1000 °C until the melt became transparent and clear. The homogenized melt solution was then cooled rapidly (50 °C/h) to the initial crystallization temperature (800 °C). It was further cooled slowly (3 °C/h) to the final crystallization temperature (700 °C) and then allowed to cool to room temperature after the furnace was turned off. The flux attached to the crystal was readily dissolved in water. Transparent and colorless $Na_2CsBe_6B_5O_{15}$ crystals (Figure S1 in the Supporting Information) are found to be moisture-stable. The powder X-ray diffraction (PXRD) patterns of grown crystals of $Na_2CsBe_6B_5O_{15}$ and the theoretical simulations from single-crystal structures match each other very well. The differences between the peak intensities for the same crystallographic index in the two patterns are believed to be caused by the preferential orientation of the powder samples (see Figure S2 in the Supporting Information). The inductively coupled plasma elemental analysis of $Na_2CsBe_6B_5O_{15}$ (Table S1 in the Supporting Information) is consistent with the compositions determined by single crystal X-ray analysis.

As shown in Figure S3 in the Supporting Information, the differential thermal analysis (DTA) curves of $Na_2CsBe_6B_5O_{15}$ exhibit only one endothermic peak starting at 866 °C upon heating to 1100 °C. The PXRD pattern of the residues reveals that $Na_2CsBe_6B_5O_{15}$ decomposes into BeO, suggesting that it

Received: May 6, 2011
Published: July 08, 2011

dx.doi.org/10.1021/ja204179g | J. Am. Chem. Soc. 2011, 133, 11458–11461

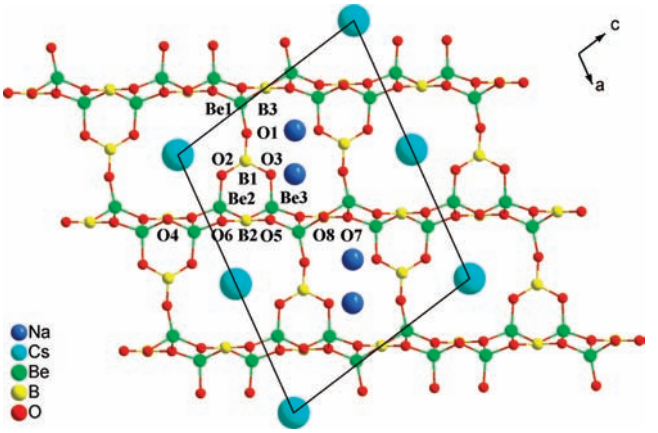

Figure 1. Crystal structure of $Na_2CsBe_6B_5O_{15}$ shown along the *b* axis.

melts incongruently. Therefore, large crystals of $Na_2CsBe_6B_5O_{15}$ must be grown with a flux and below the decomposition temperature.

UV−vis diffuse reflectance spectra were collected for $Na_2CsBe_6B_5O_{15}$ (Figure S4 in the Supporting Information). Absorption (K/S) data were calculated from the following Kubelka−Munk function:[17,18] $F(R) = (1 - R)^2/2R = K/S$, where R is the reflectance, K is the absorption, and S is the scattering. In the plots of K/S versus E, extrapolating the linear portion of the rising curve to zero provides the onset of absorption. No obvious absorption peak in the range 6.22−1.55 eV (corresponding to wavelengths of 200−800 nm) is observed for $Na_2CsBe_6B_5O_{15}$, indicating a high potential of the crystal for deep-UV NLO applications.

$Na_2CsBe_6B_5O_{15}$ crystallizes in a monoclinic crystal system with a chiral space group of *C*2. The structure as viewed along the *b* axis is illustrated in Figure 1. Each B atom is coordinated to three O atoms to form a planar $[BO_3]$ triangle, with B−O bond lengths ranging from 1.339(10) to 1.419(3) Å and O−B−O bond angles ranging from 115.6(2) to 123.6(2)°. Each Be atom is bound to four O atoms to form a distorted $[BeO_4]$ tetrahedron, with Be−O bond lengths between 1.519(4) and 1.682(6) Å and O−Be−O angles between 103.3(3) and 122.5(3)°. The 2D alveolate beryllium borate $[Be_2BO_5]_\infty$ layers in this structure are similar to those in β-$KBe_2B_3O_7$, $RbBe_2B_3O_7$, and γ-$KBe_2B_3O_7$, except that the connections between the adjacent $[Be_2BO_5]_\infty$ layers in this structure are bridged via $[BO_3]$ planar groups that lay in the *ac* plane and point in opposite directions.

Two types of tunnels exist in the 3D framework running along the *b* axis. The Na^+ and Cs^+ cations reside in these smaller and larger tunnels, respectively, where Na^+ cations are located in a seven-coordinate environment with Na−O bond lengths ranging from 2.373(2) to 2.693(2) Å and Cs^+ cations are located in an eight-coordinate environment with Cs−O bond lengths ranging from 3.230(6) to 3.453(2) Å.

The structural evolution can be illustrated through a comparison of the layer structures of KBBF, β-$KBe_2B_3O_7$, γ-$KBe_2B_3O_7$, $RbBe_2B_3O_7$, and $Na_2CsBe_6B_5O_{15}$. Although they all have similar alveolate beryllium borate layers ($[Be_2BO_3F_2]_\infty$ or $[Be_2BO_3O_2]_\infty$), the orientation periodicity of the O or F atoms bound to the Be atoms and protruding out of the layers are different. Since there is only one unique orientation of $[BO_3]^{3-}$ groups in the $[Be_2BO_3]_\infty$ layers of the aforementioned

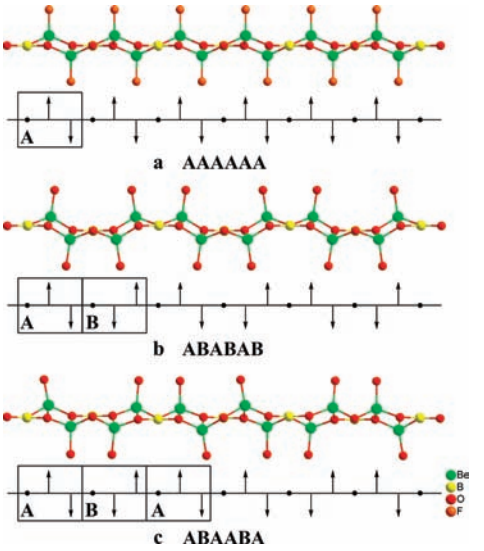

Figure 2. Comparison of $[Be_2BO_3F_2]_\infty$ or $[Be_2BO_3O_2]_\infty$ layers in (a) KBBF, (b) β-$KBe_2B_3O_7$, and (c) $Na_2CsBe_6B_5O_{15}$.

compounds, the structural differences among them are clearly illustrated when $[BO_3]^{3-}$ groups are oriented in the same direction. (Figures 2 and 3)

To realize the structural design to increase the SHG effects of these layered compounds containing alveolate networks, an ideal strategy is to construct a more compact structure through bridging the 2D layer via smaller $[BO_3]$ groups. From this a hypothesized formula is readily derived as $A_3Be_6B_5O_{15}$ (A = alkali metal) by substituting $[BO_3]$ for $[B_3O_6]$ in γ-$KBe_2B_3O_7$ when the formula is viewed as a sum of three parts, namely, cations, NLO-active 2D layers, and connectors:

$$\gamma\text{-}KBe_2B_3O_7 \times 3: \quad 3K + 3[Be_2BO_3] + 2[B_3O_6]$$

$$A_3Be_6B_5O_{15}: \quad 3A + 3[Be_2BO_3] + 2[BO_3]$$

On this basis, a target compound may be constructed by carefully arranging the framework connection and alkali-metal allocation as follows. The $[Be_2BO_3F_2]_\infty$ layer in KBBF is composed of repeating unit "A" (Figure 2a). The distance between the adjacent Be atoms that have the same Be−O bond direction (4.427 Å) is too long to bond the two O atoms from a $[BO_3]$ group (Figure 3a). In the case of β-$KBe_2B_3O_7$, meanwhile, the $[Be_2BO_3O_2]_\infty$ layer is composed of "AB" repeating units (Figure 2b). Although the aforementioned distance in this case (2.689 Å) is acceptable for binding two O atoms of a $[BO_3]$ group (Figure 3b), it is rather undesired to leave a dangling Be−O bond in the adjacent layer to which it is connected. Therefore, a reasonable configuration results from binding two O atoms of the $[BO_3]$ group to one layer and one to the other. Such configuration is herein realized in the title compound $Na_2CsBe_6B_5O_{15}$, whose $[Be_2BO_3O_2]_\infty$ layer is composed of "ABA" repeating units (Figure 2c). The resulting orientation of the $[BeO_4]$ groups and the Be−Be distance (2.559 Å) enables the $[Be_2BO_3O_2]_\infty$ layers to be bridged via $[BO_3]$ groups (Figure 1). Consequently, the orientations in the $[Be_2BO_3O_2]_\infty$ layers result in the existence of two types of tunnels, one smaller and the other bigger, between the adjacent $[Be_2BO_3O_2]_\infty$ layers. Two types of cations with different radii (i.e., Na^+ and Cs^+) are thus required to reside in these two types tunnels, respectively (Figure 1). This is

dx.doi.org/10.1021/ja204179g |*J. Am. Chem. Soc.* 2011, 133, 11458–11461

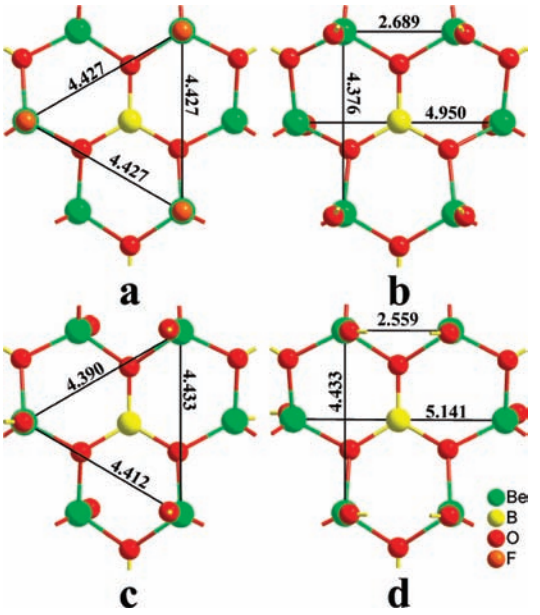

Figure 3. $[Be_2BO_3F_2]_\infty$ or $[Be_2BO_3O_2]_\infty$ layers in the structures of (a) KBBF, (b) β-$KBe_2B_3O_7$, and (c, d) $Na_2CsBe_6B_5O_{15}$.

likely the reason that we are able to find alveolate beryllium borate $[Be_2BO_5]_\infty$ layers bridged via smaller planar $[BO_3]$ groups only in binary alkaline beryllium borates and not in unitary alkaline beryllium borates.

KBBF, β-$KBe_2B_3O_7$, γ-$KBe_2B_3O_7$, $RbBe_2B_3O_7$, and $Na_2CsBe_6B_5O_{15}$ all have similar structures, and therefore, their nonlinearity originates from the same structure−property relationship. Although the layer-connector $[BO_3]$ groups in $Na_2CsBe_6B_5O_{15}$ are NLO-active building blocks, the sum of their microscopic NLO susceptibilities is close to zero because they are related by an approximate center of symmetry in this structure. In contrast, as a common character of the coplanar beryllium borate network, the $[BO_3]^{3-}$ groups in the $[Be_2BO_3]_\infty$ layers of each compound have the same orientation, which is the optimal arrangement to yield large overall NLO properties. However, the distances between adjacent layers in β-$KBe_2B_3O_7$ (8.73 Å), γ-$KBe_2B_3O_7$ (8.70 Å), $RbBe_2B_3O_7$ (8.86 Å), and KBBF (6.25 Å) are longer than that in $Na_2CsBe_6B_5O_{15}$ (6.23 Å), yielding a higher $[BO_3]^{3-}$ density for the latter. Therefore, the SHG coefficients of $Na_2CsBe_6B_5O_{15}$ are predicted to be approximately as large as those of KBBF and therefore larger than those of β-$KBe_2B_3O_7$, γ-$KBe_2B_3O_7$, and $RbBe_2B_3O_7$. Furthermore, the strong connections provided by the covalent bonds between layers mitigate drawbacks such as layer growth habit and cleavage that otherwise limit the optical applications of KBBF crystals.

SHG signals as a function of particle size obtained from the measurements made on ground crystals of $Na_2CsBe_6B_5O_{15}$ with a Q-switched Nd:YAG laser of wavelength 1064 nm are shown in Figure 4. The results are consistent with phase-matching behavior according to the rule proposed by Kurtz and Perry.[19] A LiB_3O_5 (LBO) sample was selected as a reference to ensure accurate measurements because it is the same type of optical biaxial crystal as the sample to be measured. The second-harmonic signal for $Na_2CsBe_6B_5O_{15}$l was found to be 0.55 times that for LBO. Such a value is proportional to the square of the nonlinear d_{eff} coefficient. Since the reported d_{eff} coefficient for LBO is 0.832 pm/V [2.133 times the d_{36} coefficient of potassium

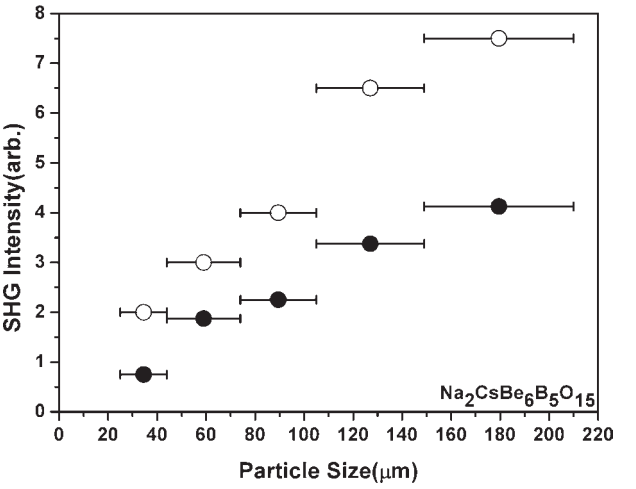

Figure 4. SHG measurements on ground $Na_2CsBe_6B_5O_{15}$ crystals (●) with LBO (○) as a reference.

Table 1. NLO Effects and Structural Characteristics of Alkaline Beryllium Borates

crystals	space group	interlayer bridging	interlayer distances (Å)	SHG coefficient[a]
KBBF[b]	$R32$	K^+-F^-	6.25	1.12
γ-$KBe_2B_3O_7$[c]	$P2_1$	$[B_3O_6]$	8.70	0.68
β-$KBe_2B_3O_7$[c]	$Pmn2_1$	$[BO_2]_\infty$	8.73	0.75
$RbBe_2B_3O_7$[c]	$Pmn2_1$	$[BO_2]_\infty$	8.86	0.79
$Na_2CsBe_6B_5O_{15}$[d]	$C2$	$[BO_3]$	6.23	1.17

[a] In multiples of d_{36}(KDP). [b] Data from ref 2. [c] Data from ref 16. [d] This work.

dihydrogen phosphate (KDP)],[20] the derived d_{eff} coefficient for $Na_2CsBe_6B_5O_{15}$ is 0.46 pm/V, which is ~1.17 times as large as that of d_{36}(KDP).

The above argumentation on structure−property correlations is in good agreement with the SHG measurements. According to the anionic group theory, the nonlinearity of $Na_2CsBe_6B_5O_{15}$ relative to that of KBBF [$1.12 \times d_{36}$(KDP)] is determined by the density of $[BO_3]^{3-}$ groups in the $[Be_2BO_3]_\infty$ layers within a unit cell, based on the same arrangement of the NLO-active $[BO_3]^{3-}$ groups. The density of the $[BO_3]^{3-}$ groups is 0.00921 per unit volume in $Na_2CsBe_6B_5O_{15}$, which is comparable to that in KBBF (0.00946). Therefore, the nonlinearity of $Na_2CsBe_6B_5O_{15}$ is calculated to be 97.4% of that of KBBF. These results agree approximately with the experimental value for $Na_2CsBe_6B_5O_{15}$, which is 1.05 times that for KBBF. The correlations between the NLO effects and structural characteristics are summarized in Table 1. As shown by this table, the nonlinearity of this type of borate containing 2D alveolate beryllium borate layers is approximately inversely proportional to the interlayer distance. Among these compounds, $Na_2CsBe_6B_5O_{15}$ possesses the largest NLO coefficient as a result of its shortest interlayer distance, which is due to the compact layer structure bridged via small $[BO_3]$ groups.

In summary, a new binary alkaline beryllium borate, $Na_2CsBe_6B_5O_{15}$, has been synthesized through spontaneous crystallization with a molten flux based on $Na_2O-Cs_2O-B_2O_3$. $Na_2CsBe_6B_5O_{15}$ consists of 2D alveolate beryllium borate $[Be_2BO_5]_\infty$ layers bridged by planar $[BO_3]$ groups. UV−vis

diffuse reflectance analysis of a powder sample of $Na_2CsBe_6B_5O_{15}$ indicates that the short-wavelength absorption edge of $Na_2CsBe_6B_5O_{15}$ is below 200 nm. Second-harmonic generation in the powder sample was measured using the Kurtz and Perry technique, which suggested that $Na_2CsBe_6B_5O_{15}$ is phase-matchable, and its measured SHG coefficient is ~1.17 times as large as d_{36}(KDP). The relatively large SHG coefficient of $Na_2CsBe_6B_5O_{15}$ likely originates from the short distance between the adjacent layers bridged by the small $[BO_3]$ groups.

■ ASSOCIATED CONTENT

Supporting Information. DTA traces, crystal pictures, PXRD patterns, diffuse reflectance absorption curves, and crystal data (CIF). This material is available free of charge via the Internet at http://pubs.acs.org.

■ AUTHOR INFORMATION

Corresponding Author
nye@fjirsm.ac.cn

■ ACKNOWLEDGMENT

This work was supported by the National Natural Science Foundation of China (50872132 and 90922035). The authors thank Prof. R. G. Xiong and X. Y. Chen for the measurement of the temperature-dependence of the SHG.

■ REFERENCES

(1) Mei, L. F.; Wang, Y. B.; Chen, C. T. *Mater. Res. Bull.* **1994**, *29*, 81.
(2) Mei, L.; Huang, X.; Wang, Y.; Wu, Q.; Wu, B.; Chen, C. *Z. Kristallogr.* **1995**, *210*, 93.
(3) McMillen, C. D.; Kolis, J. W. *J. Cryst. Growth* **2008**, *310*, 2033.
(4) Chen, C. T.; Luo, S. Y.; Wang, X. Y.; Wang, G. L.; Wen, X. H.; Wu, H. X.; Zhang, X.; Xu, Z. Y. *J. Opt. Soc. Am. B* **2009**, *26*, 1519.
(5) McMillen, C. D.; Hu, J.; VanDerveer, D.; Kolis, J. W. *Acta Crystallogr., Sect. B* **2009**, *65*, 445.
(6) Chen, C. T.; Wang, Y. B.; Wu, B. C.; Wu, K. C.; Zeng, W. L.; Yu, L. H. *Nature* **1995**, *373*, 322.
(7) Qi, H.; Chen, C. T. *Inorg. Chem. Commun.* **2001**, *4*, 565.
(8) Qi, H.; Chen, C. T. *Chem. Lett.* **2001**, 352.
(9) Pan, S.; Smit, J. P.; Watkins, B.; Marvel, M. R.; Stern, C. L.; Poeppelmeier, K. R. *J. Am. Chem. Soc.* **2006**, *128*, 11631.
(10) Chang, H. Y.; Kim, S. H.; Halasyamani, P. S.; Ok, K. M. *J. Am. Chem. Soc.* **2009**, *131*, 2426.
(11) Chang, H. Y.; Kim, S. H.; Ok, K. M.; Halasyamani, P. S. *J. Am. Chem. Soc.* **2009**, *131*, 6865.
(12) Chang, H. Y.; Kim, S. H.; Ok, K. M.; Halasyamani, P. S. *Chem. Mater.* **2009**, *21*, 1654.
(13) Sun, C. F.; Hu, C. L.; Xu, X.; Ling, J. B.; Hu, T.; Kong, F.; Long, X. F.; Mao, J. G. *J. Am. Chem. Soc.* **2009**, *131*, 9486.
(14) Halasyamani, P. S.; Poeppelmeier, K. R. *Chem. Mater.* **1998**, *10*, 2753.
(15) Wu, H. P.; Pan, S. L.; Poeppelmeier, K. R.; Li, H. Y.; Jia, D. Z.; Chen, Z. H.; Fan, X. Y.; Yang, Y.; Rondinelli, J. M.; Luo, H. S. *J. Am. Chem. Soc.* **2011**, *133*, 7786.
(16) Wang, S. C.; Ye, N.; Li, W.; Zhao, D. *J. Am. Chem. Soc.* **2010**, *132*, 8779.
(17) Kubelka, P.; Munk, F. *Z. Tech. Phys* **1931**, *12*, 593.
(18) Tauc, J. *Mater. Res. Bull.* **1970**, *5*, 721.
(19) Kurtz, S. K.; Perry, T. T. *J. Appl. Phys.* **1968**, *39*, 3798.
(20) Roberts, D. A. *IEEE J. Quantum Electron.* **1992**, *28*, 2057.